UNIVERSITY OF CALIFORNIA, SAN DIEGO
SCRIPPS INSTITUTION OF OCEANOGRAPHY
VISIBILITY LABORATORY
LA JOLLA, CALIFORNIA 92093

# OPTICAL REMOTE SENSING IN THE NEW YORK BIGHT

**Wayne H. Wilson**

**SIO Ref. 78-27**
**October 1978**

Sponsored by
U. S. Department of Commerce
National Oceanic and Atmospheric Administration
National Environmental Satellite Service
Grant No. 04-6-158-44033

Approved:

James L. Harris, Sr., Director
Visibility Laboratory

Approved:

William A. Nierenberg, Director
Scripps Institution of Oceanography

## ABSTRACT

Ocean color remote sensing experiments were conducted in the New York Bight area during April 1975. Concurrent measurements were made by a U-2 carrying the Ocean Color Scanner developed at NASA/Goddard Space Flight Center and surface vessels collecting in-situ data.

Analysis of the imagery from the Ocean Color Scanner has been made and methods developed to extract hydro-optical properties from the apparent radiances measured by the scanner.

Relationships between the water reflectances and chlorophyll concentration have been developed and their use in the present study analyzed.

The good correlations between the measured chlorophyll values and the derived ones illustrate the feasibility of the methods used and their use with other waters or times.

## INTRODUCTION

The National Oceanic and Atmospheric Administration (NOAA) for the last several years has sponsored a program to obtain environmental information in selected marine locations. This program, Marine Ecosystem Analysis (MESA), chose the heavily impacted New York Bight area for the first intensive studies. The goals of the program are to develop techniques for monitoring and predicting man's effects on the marine environment and to provide guidance for development and conservation of these areas.

In order to provide rapid and efficient monitoring techniques, the National Environmental Satellite Service (NESS) of NOAA has conducted studies in the applicability of remote sensing technology to these efforts. In particular NASA was requested to participate in a cooperative program aimed at defining and evaluating the methodology in which remote sensors would be employed in conjunction with surface measurements to study and interpret marine processes.

The first project of this effort was an intensive study in the New York Bight during the period April 7-17, 1975. Six experiments, utilizing different aircraft mounted remote sensors, were conducted by NASA. At the same time NESS acquired in-situ surface data from surface vessels and helicopters.

The purpose of this report is to discuss and analyze the data obtained from one of the remote sensors, the Ocean Color Scanner (OCS). Specifically, techniques of utilizing the apparent radiances measured by the OCS to obtain inherent surface radiances and also surface chlorophyll and sediment concentration have been investigated and will be reported on. The correlation of these derived properties with the actual in-situ measurements will be made and discussed.

## EXPERIMENTAL DESCRIPTION

Ocean Color Scanner

The Ocean Color Scanner was flown on a NASA U-2 aircraft at an altitude of 19.8 km (65,000 ft.), on April 9, 13 and 14, 1975 over the New York Bight area. Because of equipment failure, the data from April 14 was lost. The April 9th flight yielded data but concurrent in-situ surface truth was not obtained. The experiment on April 13 was very successful in terms of good remote data and also a substantial in-situ data base. This report has concentrated on this latter day.

The OCS is a 10-channel multispectral scanner with wavelengths centered in the region 433 to 772 nanometers (Table 1). The nominal bandwidth of each channel is 22 nm. The scanner is pointed to the nadir and scans perpendicular to the flight direction of the aircraft. The nominal scan angle is 45° to either side of the nadir. The spatial resolution is 3.8 milliradians. This yields a resolution on the ground of approximately 75 meters with a sensor altitude of 19.8 km. The scan rate is such that the forward motion of the aircraft per scan line approximately equals the ground resolution. Thus the scan lines are essentially adjacent to one another. They are actually at intervals of about 79 meters.

The sampling rate during one scan line was such that there was only approximately 260-270 samples in the 90° nadir scan. This yields an undersampling in the cross track direction. Adjacent samples were approximately spaced at intervals of 115 meters at the nadir and further apart away from the nadir. The equiangular sampling introduces a geometric distortion in the sense that an image made directly from the data will not be an equal area mapping. For comparison with normal maps and for display purposes, the distortion is easily rectified by interpolating the radiance values at equal distance increments.

The radiance data from the OCS may be digitized in the air and/or recorded in analogue form for later digitization. The data is digitized

to 10 bits. The gain of each channel may be varied by factors of x1, x1.5, x2, and x3. These gains are adjusted before the flight and are chosen for optimum recording of the radiance from the sea surface.

TABLE I

| Channel | Wavelength [nm] | Bandwidth [nm] | Saturation Radiance - $N_s$ ($\mu$watts/cm$^2$-nm) |
|---|---|---|---|
| 1 | 433 | 22.5 | 40.1 |
| 2 | 471 | 21.5 | 26.0 |
| 3 | 509 | 27.5 | 23.6 |
| 4 | 547 | 24.5 | 14.7 |
| 5 | 583 | 25.0 | 11.8 |
| 6 | 620 | 26.0 | 10.0 |
| 7 | 662 | 22.0 | 7.55 |
| 8 | 698 | 20.5 | 5.0 |
| 9 | 733 | 22.5 | 11.9 |
| 10 | 772 | 23.0 | 3.47 |

(From Hovis & Leung)

The flight direction of the aircraft is usually toward or away from the sun.

The data available for the 13th of April consisted of a single flight line with a total of 2340 scan lines. The flight started approximately 100 nautical miles southeast of the Hudson River entrance and ended at the entrance to the river. The flight track began at 1045 EDT and ended at 1100 EDT. From this time information and the geographic location, the solar zenith and azimuth angles were computed. At the start of the track these were 41°27' zenith angle and 129° azimuth. At the end 40°54' zenith and 132°30' azimuth. For further computation the values of 41° zenith and 132° azimuth were assumed. Because the aircraft flew directly over a cloud as it was nearing the river entrance and the cloud's shadow

was directly in line with it, the flight direction of the aircraft was assumed to be 308°.

The first eight channels were available in digitized form. Figure 1 is the image of the raw data of the full flight track for channel 4.

## Surface Data Collection

During the period of April 7 to April 16, the NOAA ship GEORGE B. KELEZ collected oceanographic data in the New York Bight area. The data was collected and reduced by D. Clark, H. Stumpf, L. Strees, and S. Roman of NESS, J. Gattone of the U.S. Naval Oceanographic Office, D. Kiefer of Scripps Institution of Oceanography, W. Glidden of National Marine Fisheries Services and T. Nelson of Atlantic Oceanographic and Meteorological Laboratories. The KELEZ stations were supplemented by helicopter data collection operations on several days. On April 13 the KELEZ ran a track line of about 50 n. miles and occupied six stations. The track began at 0800 EDT and ran until 1550 EDT. The tide at Sandy Hook, New Jersey, had a high at 0818 EDT and a low at 1442 EDT. Thus during most of the data taking the tide was going out. The six stations were occupied at the times given in Table II.

TABLE II

| Ship Station | Time [EDT] |
|---|---|
| 3.1 | 0835 |
| 3.2 | 0945 |
| 3.3 | 1110 |
| 3.4 | 1235 |
| 3.5 | 1419 |
| 3.6 | 1525 |

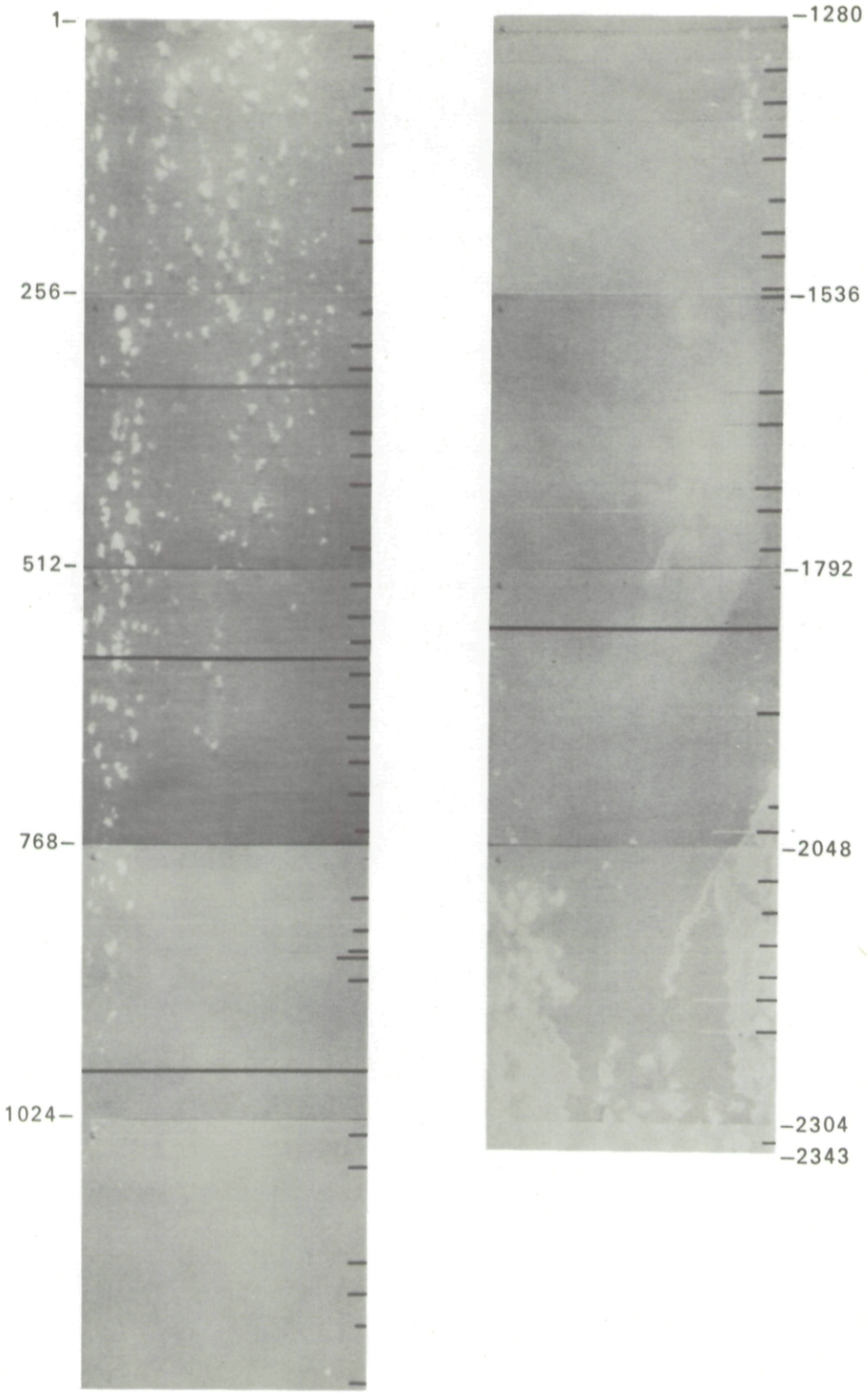


Fig. 1. Raw image from tape of band 4 (547 nm). Scan lines from the beginning of the flight line are indicated along the edges of the image. The numerous "bad" lines can be observed as either short, shifted or absent. The image has not been corrected for the distortion caused by equiangular sampling.

During the over flight of the U-2, the KELEZ was in the region of station 3.3. Figure 2 is a map of the Bight area with the stations and track line indicated. Also on the map are the 31 stations that the helicopter made. Some of these were not in the area viewed by the OCS, and are therefore not plotted. The map also has the flight line of the U-2 and the boundaries of the scan from the OCS.

The data collected by the KELEZ included salinity, temperature, beam transmittance, secchi disk depth, chlorophyll a, and suspended particulate size distribution. An attempt was also made to measure downwelling and upwelling surface irradiance.

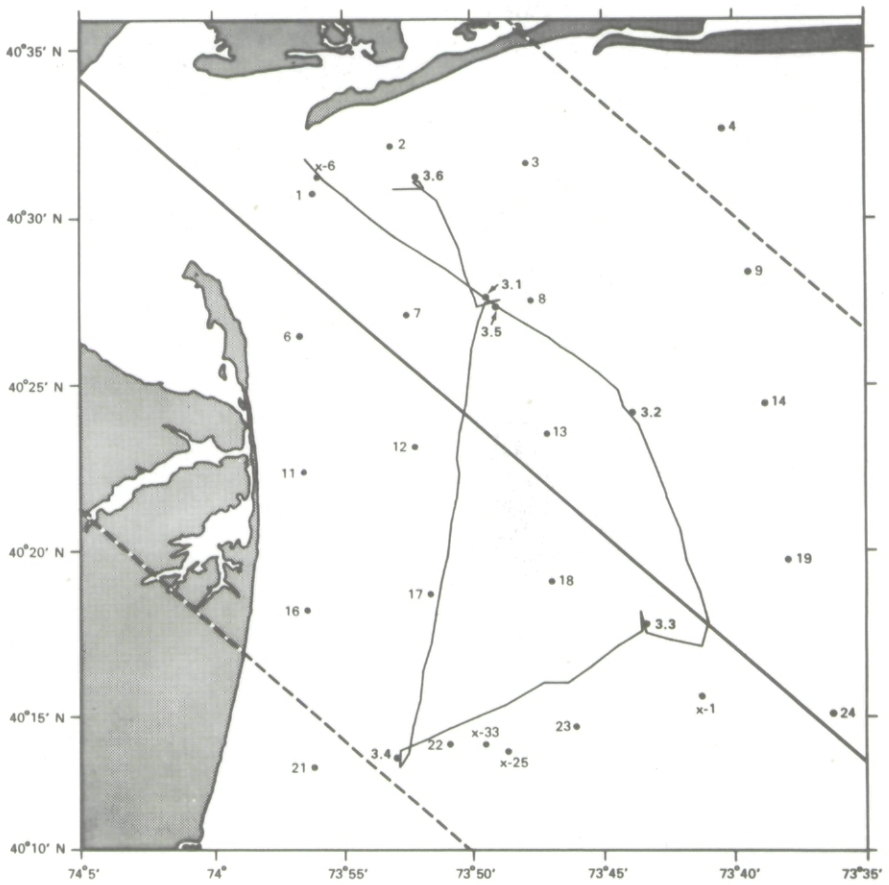


Fig. 2. Map of the New York Bight area. The solid line crossing the map from lower right to upper left is the ground track of the U-2 flight. The two dashed lines paralleling this track are the approximate boundaries of the OCS imagery. The individual points are the stations at which samples were obtained by helicopter. The track of the GEORGE KELEZ on 13 April is also indicated along with the positions of stations 3.1 to 3.6.

The beam transmittances for three of the stations are shown in Figure 3. The transmissometer was filtered with a Wratten 61 filter and peaked around 530 nm with a bandwidth of about 50 nm. The transmittance as shown in Figure 3 was typically of the order of 20%/meter or less in the top 10 meters. Comparison of the profiles of station 3.1 and 3.5 which were taken approximately in the same place but 5.5 hours apart illustrates the changes which were occurring in the area during the data taking. Station 3.1 taken near high tide has a layer of clear water in the top meter. By the afternoon (Station 3.5) at low tide, the transmission had dropped from 12%/meter to 8%/meter, a change in the volume attenuation coefficient of 16%.

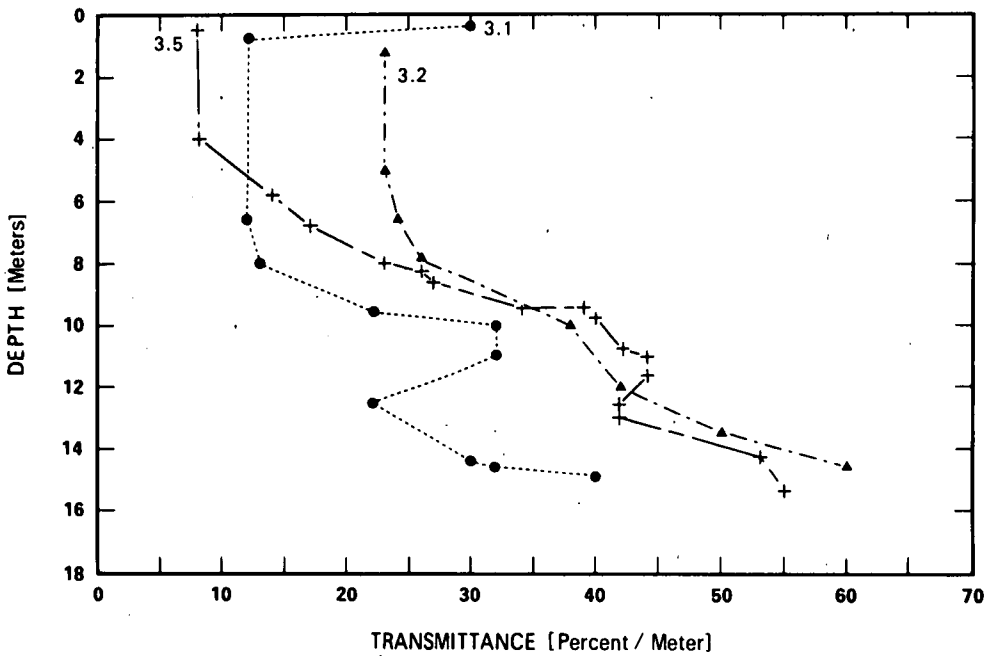


Fig. 3. Plot of the transmittance versus depth of three (3) of the KELEZ'S stations.

This change indicates one of the problems of taking synoptic measurements such as from the OCS and relating them to measurements made from surface vessels over a period of time when the local environment is in a state of flux.

The secchi disk depths for the stations as indicated in Table III along with the beam transmittance values indicate that the reciprocal diffuse attenuation coefficient, $K^{-1}$, was on the order of several meters.

TABLE III

| Station | Secchi Depth |
|---|---|
| 3.1 | 2.5 |
| 3.2 | 4.25 |
| 3.3 | 3.5 |
| 3.4 | 5.0 |
| 3.5 | 4.0 |
| 3.6 | 1.7 |

Since $K^{-1}$ defines the depth from which 90 percent of the remote sensed signal originates (Gordon and McCluney), this indicates that the remote signal obtained at altitude was essentially that which was produced by a surface layer several meters thick. Any sub-surface layer phenomenon was hidden from view of the remote sensor and could not be monitored in the Bight during the experiment by the OCS.

Chlorophyll-a concentrations were calculated by measuring the chlorophyll-a fluorescence. On station, profiles of in-situ chlorophyll-a fluorescence were made by lowering a submerged pump which supplied water to a Turner III fluorometer. Discrete samples were taken and their chlorophyll-a concentrations determined by the extraction method. Thus the ratio of chlorophyll-a to fluorescence for the particular station could be obtained. During transit between stations continuous measurements of in-situ fluorescence were made and the ratios of chlorophyll-a to fluorescence linearly interpolated in order to obtain the chlorophyll concentrations.

Water samples collected by the helicopters at their stations were later processed by the extraction technique for chlorophyll-a.

Again, comparing stations 3.1 and 3.5 with respect to the fluorescence and chlorophyll-a profiles shown in Figure 4, significant changes

occurred over the space of 5.5 hours. In the case of fluorescence at the surface, increases of almost 100% occurred while the chlorophyll-a increased by 16%. Dr. Kiefer who took the samples interpreted this difference to be due to a noticeable amount of photoinhibition of the fluorescence taking place in the surface waters (Kiefer). It should be noted that the increase of chlorophyll-a concentration parallels the corresponding increase detected in the attenuation coefficient discussed above. This would suggest that the changes in the transmission were caused by the increase of the phytoplankton population which resulted in an increase of chlorophyll-a.

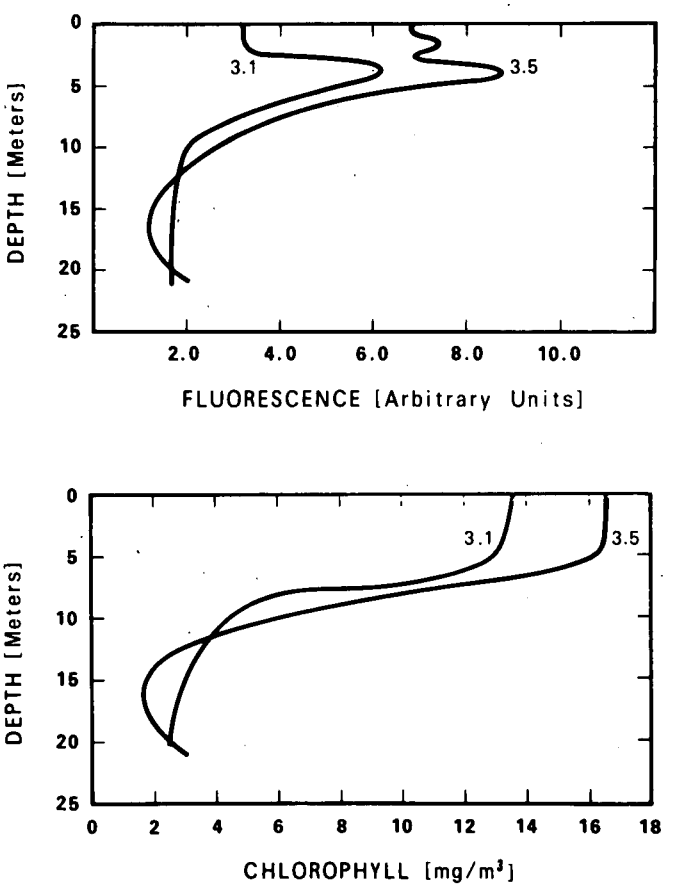


Fig. 4. Top figure is the fluorescence versus depth obtained at the stations 3.1 and 3.5. These stations were approximately at the same position but were held 5½ hours apart. The depth profile was obtained by lowering a hose and pumping water up through a Turner fluorometer located on the KELEZ.

The bottom figure are plots of the chlorophyll-a concentration obtained from the above fluorometric data and calibrated by discrete samples analyzed by the extraction method.

Suspended particulates were measured with a Coulter counter from samples drawn from the in-situ pump described above for the chlorophyll-a studies. The helicopter-collected samples were analyzed for concentrations and size distributions.

Location of the helicopter stations was determined by an on-board Loran-A system. Position accuracy was estimated at ±200 meters or better. (i.e., 2 to 3 pixels on the OCS images).

One measurement of above surface downwelling irradiance, was obtained on April 13 at Station 3.3 at 1122 EDT. This was approximately a half hour after the U-2 over-flight. There were difficulties in operating the spectroradiometer due to ship power variations and this measurement was the only one considered satisfactory.

There was one meteorological observation made at the Ambrose Light Station on April 13, 1975. At 0900 the wind was 14 knots from 310°. The National Weather Service reported from John F. Kennedy International Airport for April 13 that the visibility was 32 km between 1000 and 1300 EDT and the wind was 12-16 knots from 300° to 320°.

## OCS DATA PROCESSING

Before processing the imagery from the OCS for April 13, some editing was required. All of the channels had bad lines like those in Figure 1. These seemed to be either dropped lines, scans which started too soon or ones which ended too soon. Probably 90% of the bad lines occurred in all channels. The remaining were found in only one or two. The bad lines were removed by averaging the two adjacent ones and inserting the average into the image. No lines were removed completely. This procedure was followed because of the lack of location information for each scan line. If lines are dropped arbitrarily, scan lines far from known landmarks may be positioned a considerable distance from where they are actually located. The only reference to the location of some

features such as the acid dump (Figure 1, Line 1792) is the number of scan lines to a known point such as Sandy Hook on the New Jersey coast.

After this filtering a subsection of 768 lines from line 1501 to 2268 was extracted from each of the 8 channels and this set was used for further processing. A section of 256 lines were also taken from line 1001 to 1256. This latter section as seen in Figure 1 is clear of any clouds and noticeable ocean features.

Histograms of each of the eight channels from lines 1501 to 2268 were made and are shown in Figure 5. These are plots of the number of pixels in each image having a common value. These are useful for digitization quality and instrument gain assessment. They are also used to provide information for various enhancement techniques. The set of images in Figure 6 of the eight channels have been enhanced by clipping at the lowest and highest meaningful value as indicated in Figure 5.

It should be noted in Figure 5 that channels 1, 2, 3 and 8 seem to have different gain settings or calibrations than the other four channels. These higher gain settings, especially for channels 1 and 2, lead to a significant loss of radiometric resolution. For the purposes of using these channels for chlorophyll algorithm development, this loss severely limits the usefulness of these channels.

In the images of Figure 6, a common characteristic is a general increase in brightness along the edge of the scan and also down the center. If the average scan line is computed, for example in channel 8 in the region of the acid dump, these increases are very definite (Figure 7). The edge brightness increase is due to the increase in path radiance while the center increase may be shown due to sun glitter off the water. Because of the anomaly of the acid dump affecting the symmetry of the averaging of scan lines, the section previously mentioned from lines 1001 to 1256 was used to investigate the path radiance and glitter.

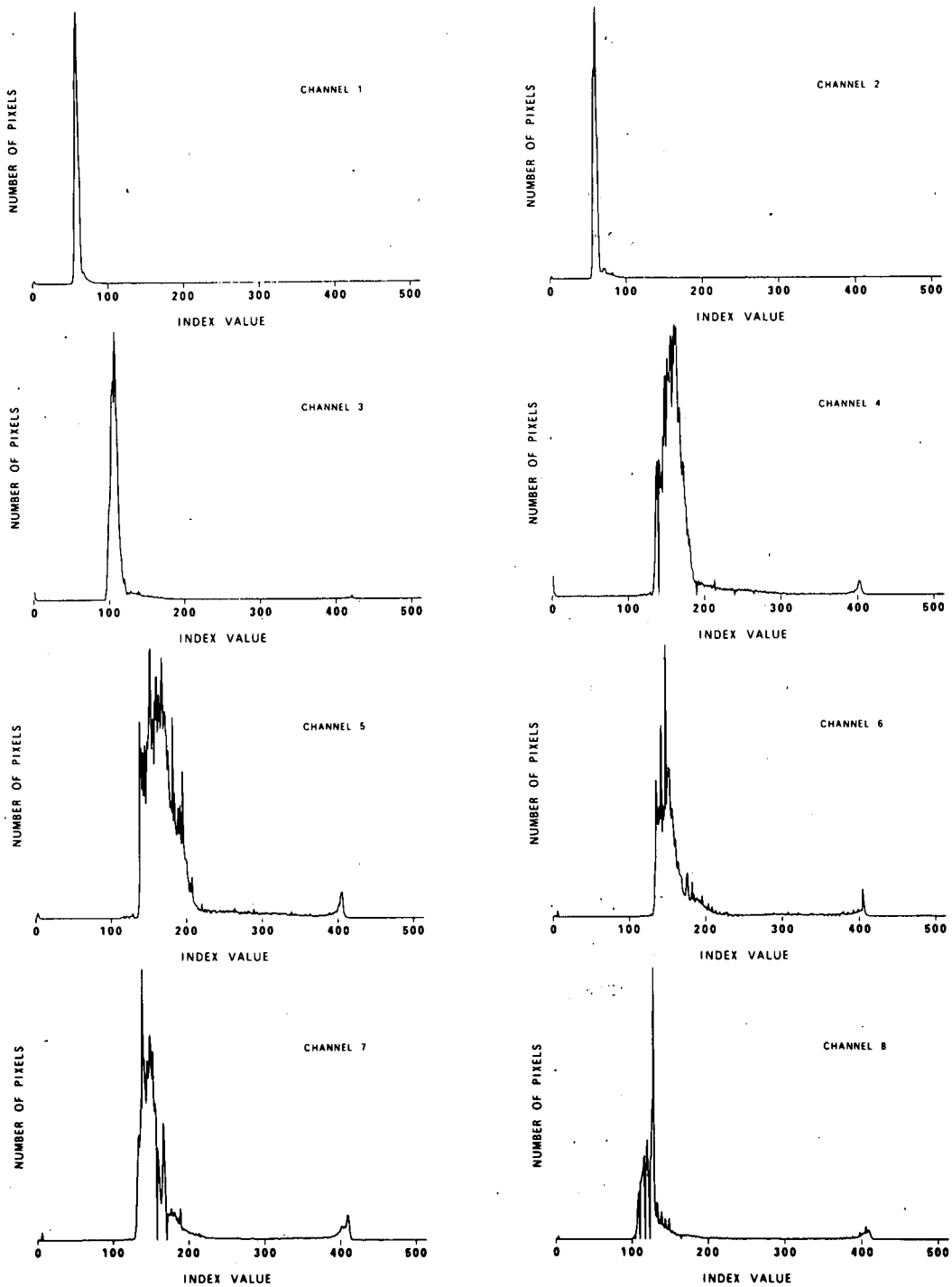


Fig. 5. Histograms of the number of pixels in the imagery for each band having the same index value. The OCS digitizes the radiance readings at 1024 levels with saturation occuring approximately at a level of 410. Channels 1 and 2, and possibly 3 and 8, were operated with different gain levels than the other channels. This led to higher noise levels and less radiometric resolution in these channels as compared with the other bands.

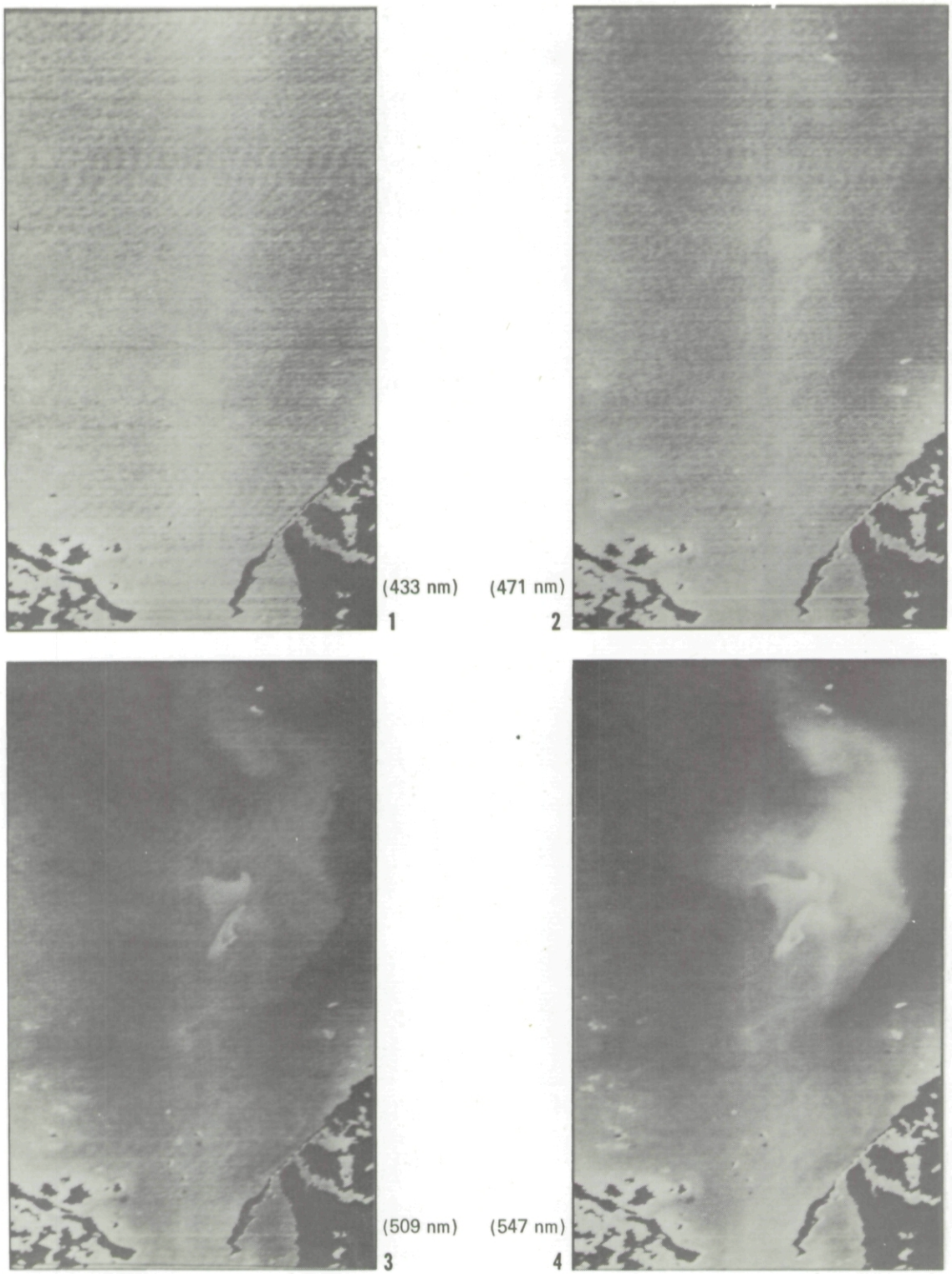


Fig. 6a. Images of channels 1, 2, 3, and 4. These have had the "bad" lines corrected and the angular distortion eliminated. The numbers by the images indicate the channel number.

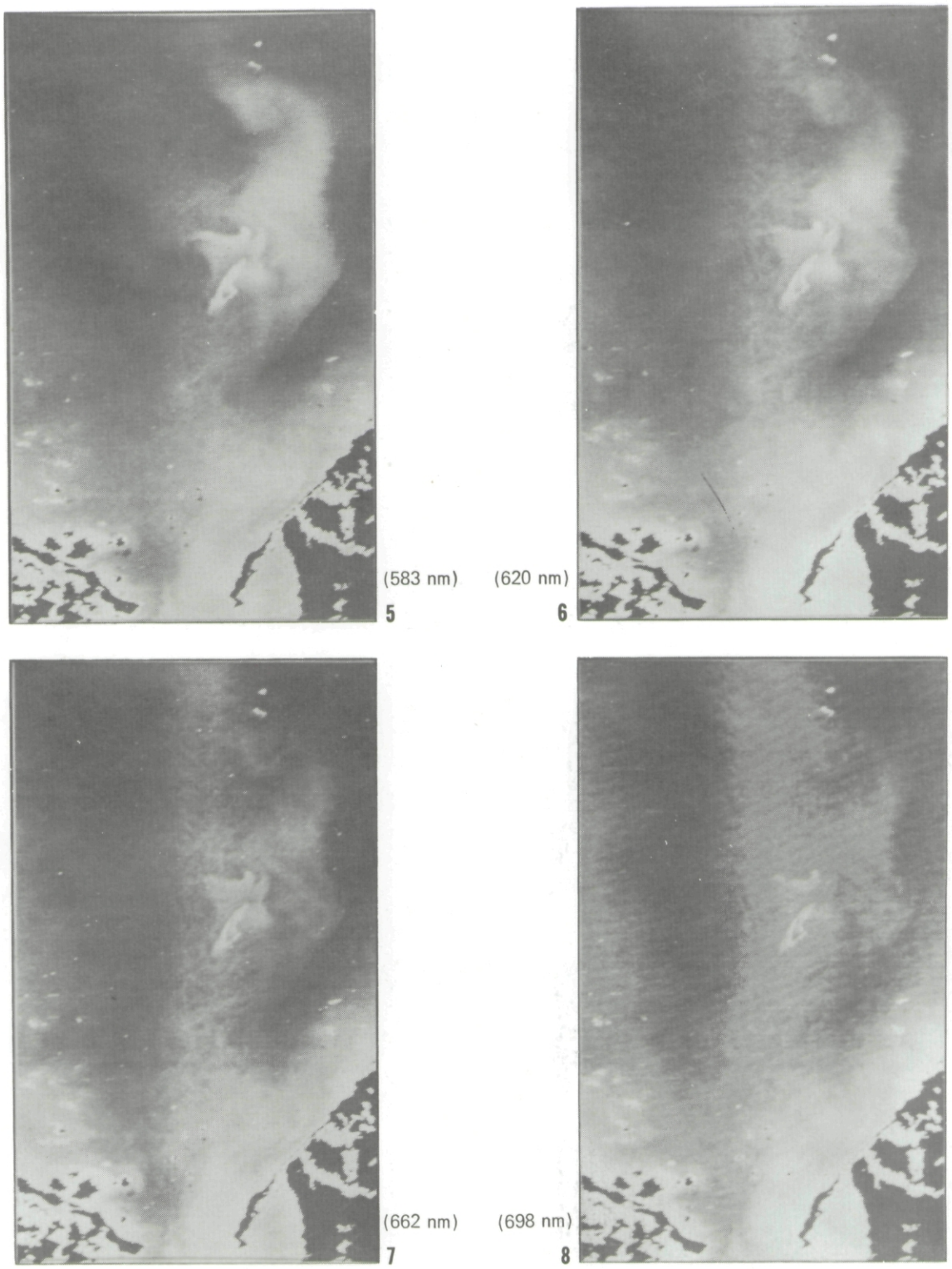


Fig. 6b. Images of channels 5, 6, 7, and 8. These have had the "bad" lines corrected and the angular distortion eliminated. The numbers by the images indicate the channel number.

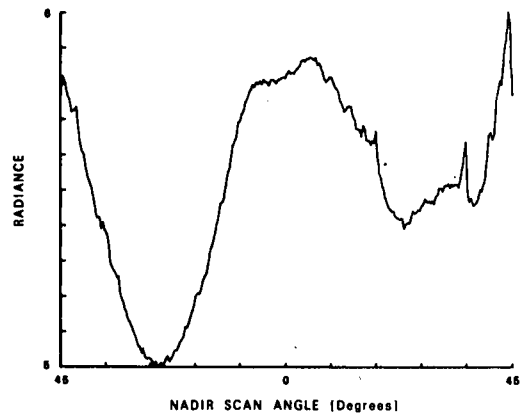


Fig. 7. The average scan line from channel 8 in Fig. 6 in the region of the acid dump.

The average scan line for the section of the imagery from lines 1001 to 1256 for each of the channels was computed and multiplied by the calibration factors obtained with the OCS tape. The nadir radiance value for each channel was then plotted versus wavelength. These radiances are plotted in Figure 8 as the top bold curve labeled A. From predictions made by a radiative transfer model for the atmospheric properties for 13 April it was felt that the radiance values from the OCS rose much faster in going toward the blue wavelengths than would be expected. If the atmospheric transmission in the radiative transfer model was decreased in order to increase the path radiance which would in turn increase the apparent nadir radiance at altitude, the observed increase in the nadir direction (see Figure 7) due to sun glitter was completely eliminated. The lower transmission values were also completely unrealistic in terms of the observed visibility of 32 km.

This investigation led to the belief that the calibration factors were possibly wrong. The factors used were obtained from the OCS tape. These had units of $\mu$ watts/cm$^2$/nm per index value. To obtain apparent radiances from the values on the tape, these factors were divided by $\pi$ to convert to radiance units and channels 1 and 2 multiplied by 1.79 and channel 3 by 1.12. If these resultant factors were plotted versus wavelength and compared with the published saturation radiance values from

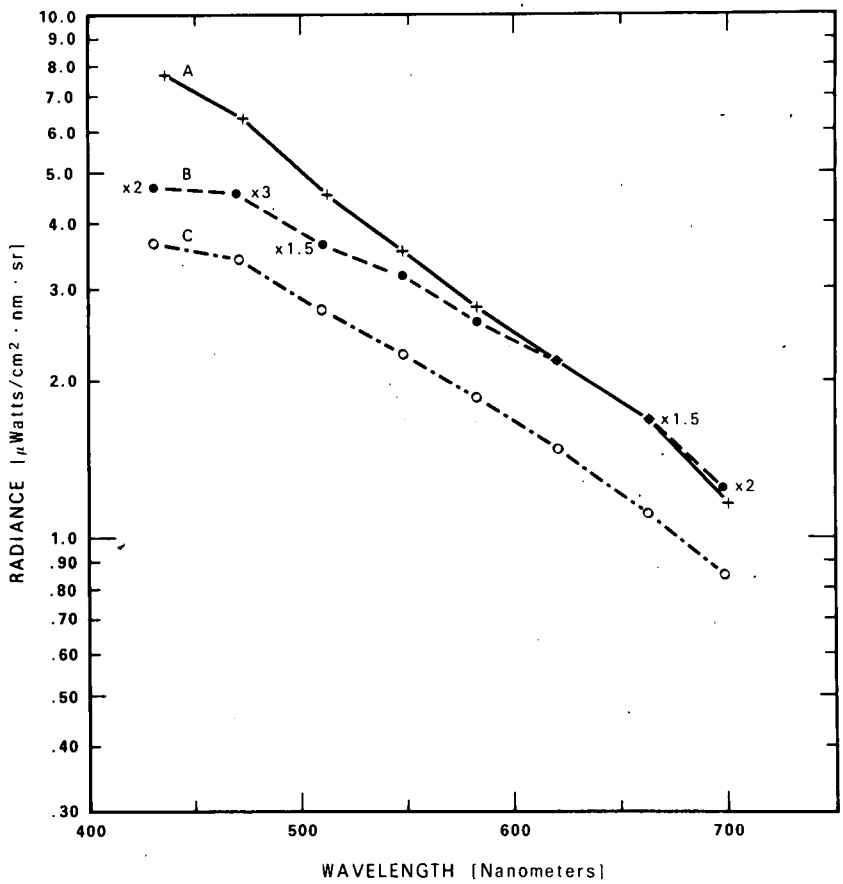


Fig. 8. The apparent radiance of the nadir for the average scan line of lines 1001 to 1256 from Fig. 1. Curve A is the apparent radiance computed using calibration factors obtained from the OCS tape. Curve B is the apparent radiance computed from new calibration factors obtained by comparison of old factors with published saturation values. The values next to the individual channels on curve B are the assumed gains of the OCS for the April 13th flight. Channels 3 through 7 are all at x1.5 gain. Curve C is the predicted path radiance computed by the RADSEA program.

Table I, the curves were not parallel on semi-log paper (Note: the values from Table I are described as radiance values but are given in units of irradiance. If they are actually irradiances, they must be divided by $\pi$ to convert them to radiances).

The assumptions were then made that the calibration factors are directly proportional to the saturation values, and that the original calibration factors from the OCS were correct in the red region of the spectrum. (i.e., channels 6 and 7). By taking the ratio of the old calibration to the saturation values for channels 6 and 7 and then applying this ratio to all channels, a new calibration curve was computed.

The observed nadir index values were then multiplied by these new factors to obtain apparent radiances and plotted in Figure 8 as curve B. It was noted that channels 1, 2 and 8 did not fall on a smooth curve as one might expect. If the assumption that the calibration factors are valid for a gain of x1.5 (in general the OCS has been calibrated with a gain of x1.5) then changing the gain of channel 1 to x2, channel 2 to x3 and channel 8 to x2, produces values for the apparent radiance as indicated in Figure 8, curve B. The assumed gains are indicated for each channel.

Since those computations were made, information has been received that there is doubt of the validity of the old calibration factors. At the present there is some question if the true calibration for the April 13th flight can be recovered. Though there are many questions concerning the derivation of the new calibration factors, the fact that they produce reasonable values for the apparent radiance in terms of the known atmospheric and oceanic optical properties for the 13th of April suggests that they are not too far wrong. The good correlation with the predictions made by the radiative transfer model supports this contention.

Using the new factors, the radiances for the average scan lines were computed and are plotted in Figure 9.

The observation should be made that the average scan line is slightly assymmetric, the values tending to be higher on the right edge. This would indicate an increase in path radiance in this direction which is looking toward the New Jersey Coast. This increase in path radiance is a result of a decrease in atmospheric transmittance due to higher concentrations of particulate matter in the atmosphere.

Using a computer program written at the Visibility Laboratory called RADSEA (Wilson), the apparent radiance of the ocean at the aircraft altitude was computed. Since there were only estimates of the parameters affecting the apparent radiance signal (i.e., atmospheric transmittance, wind speed, atmospheric volume scattering function), a modified least squares fit of the measured apparent radiances was made. This involved

varying the above mentioned parameters until the predicted apparent radiances for all channels yielded the best fit to the measured apparent radiances. The predicted apparent radiances are plotted in Figure 10. Comparison with the measured radiances in Figure 9 shows close correlation for all channels.

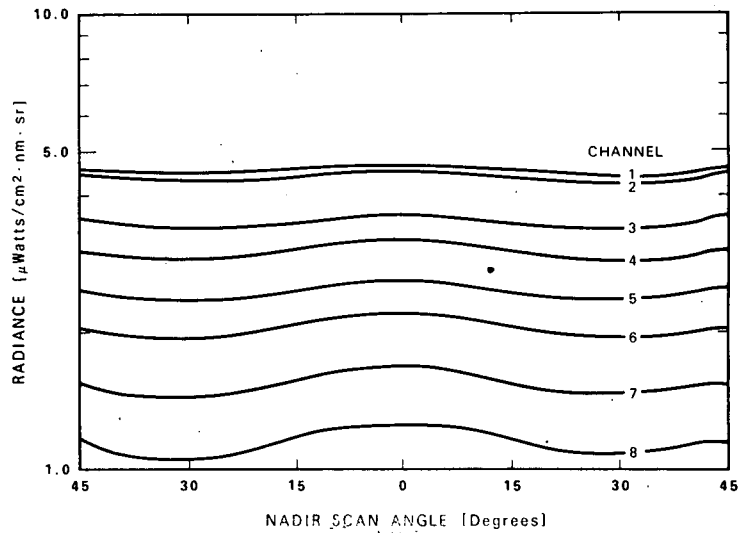


Fig. 9. The apparent radiances for the average scan line between 1001 and 1256 for each of the channels.

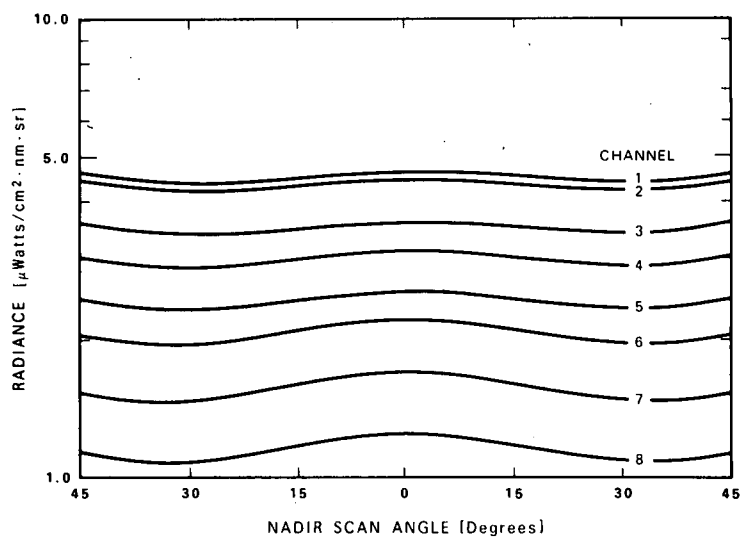


Fig. 10. The apparent radiances for each channel computed from the program RADSEA with wind speed of 7.7 m/sec (15 knots) and assumptions about the atmospheric transmittance and average water reflectance.

The RADSEA program utilizes the model for a clear atmosphere proposed by Gordon (Gordon, 1969, 1970) for the prediction of the atmospheric optical properties. The derived vertical path transmittance from earth-to-space as a function of wavelength obtained by the fitting procedure is plotted in Figure 11.

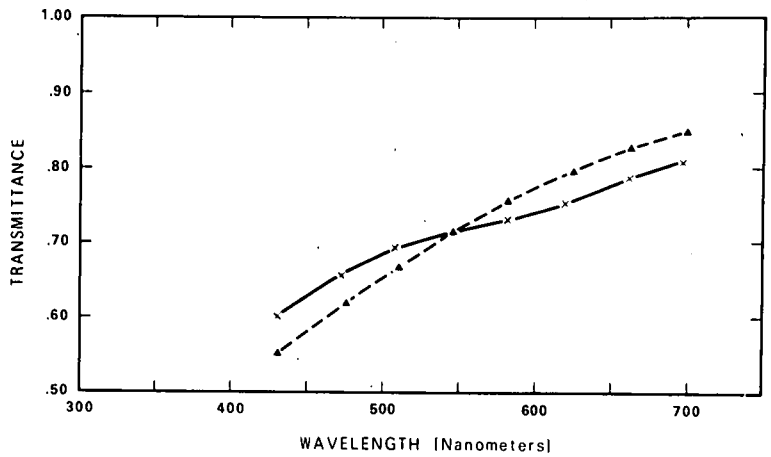


Fig. 11. Transmittance of vertical path of sight through the whole atmosphere. The solid curve is the derived transmittance by the best fit of the observed apparent radiance to the predicted apparent radiances in Figures 9 and 10. The dashed curve is the predicted transmittance from LOWTRAN 3 program for a surface visibility of 32 km.

A visibility of 32 km, used as an input into the LOWTRAN3 program which computes atmospheric transmittance, yields the comparison curve (Selby & McClatchey). A method of measuring atmospheric transmittance rather than relying on visibility estimates would help considerably in performing the calculations described here.

The best fit for the wind speed was 7.7 m/sec (15 knots).

The solar irradiance outside the atmosphere was obtained from Thekaekara. The total downwelling irradiance at the surface predicted by the modeling is plotted in Figure 12 along with the irradiance measured on board the KELEZ. The predicted irradiance is consistently higher than that measured but the reason is unknown. There is some reason to believe, however, that the measured irradiance values are in error due to the considerable problems experienced with the instrument.

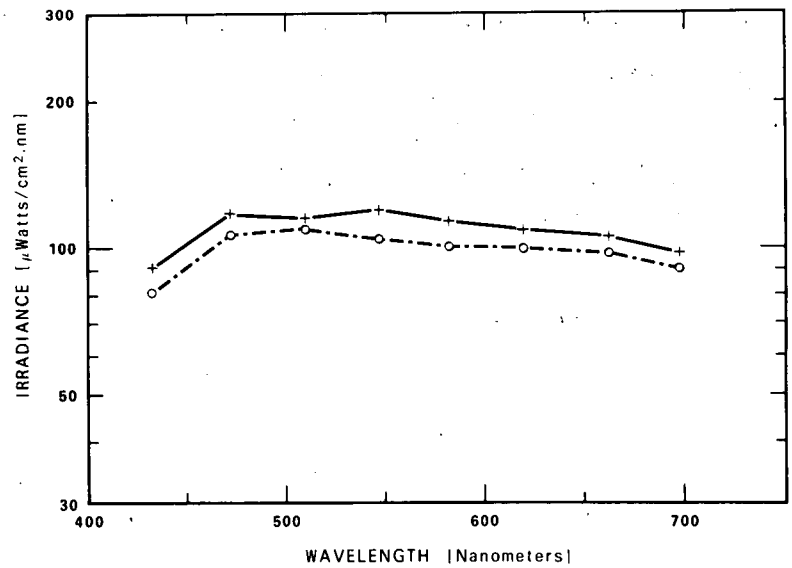


Fig. 12. The total downwelling irradiance at the ocean surface for 1120 EDT, 13 April. The solid line is that predicted from the RADSEA pro-ram. The dashed curve is the irradiance measured on board the KELEZ.

Using the parameters derived (i.e., wind speed, atmospheric transmittance, etc.) calculations were made for each channel to compute the subsurface irradiance reflectance, R, of the water column for each pixel in the images in Figure 6.

In general the apparent radiance, $N_z$, sensed at an altitude z is composed of two parts, one the path radiance, $N^*$, and second the transmitted signal from the ocean itself, $N_o$.

Thus

$$N_z = N^* + N_o T ,$$

where T is the atmospheric transmittance. $N_o$ is further composed of components due to sun glitter, $N_g$, sky reflectance, $N_{sky}$, and the actual signal from the water $N_w$, thus

$$N_o = N_g + N_{sky} + N_w .$$

$N_w$ may be further expressed as

$$N_w = H_{total} \frac{B'}{Q} \cdot R \ ,$$

where $H_{total}$ is the downwelling irradiance just above the water surface, and B' is a factor describing the transmittance of irradiance down into the water and the transmittance of radiance up through the surface. Q is a factor describing the ratio between the irradiance exiting from a substance and the radiance exiting from it.

For a Lambertian reflector

$$N = \frac{H}{\pi} \ ,$$

so in this case $Q = \pi$; however, studies by Austin at the Visibility Laboratory (Duntley, et. al.), have shown that Q is more on the order of 5.0-5.2 for natural water.

R is the irradiance reflectance of water normally defined as

$$R = \frac{H_{up}}{H_{down}} \ .$$

In the present calculation the quantity of interest is R. Therefore

$$R = \frac{Q}{B' H_{total}} \times \left[ \frac{(N_z - N^*)}{T} - (N_g + N_{sky}) \right]$$

The program RADSEA described earlier yielded the values for all the quantities on the right side except for the apparent radiance $N_z$ which came from the OCS imagery.

The computed reflectances for Stations 3.1-3.5 are plotted in Figure 13. Further discussion of this figure will occur below.

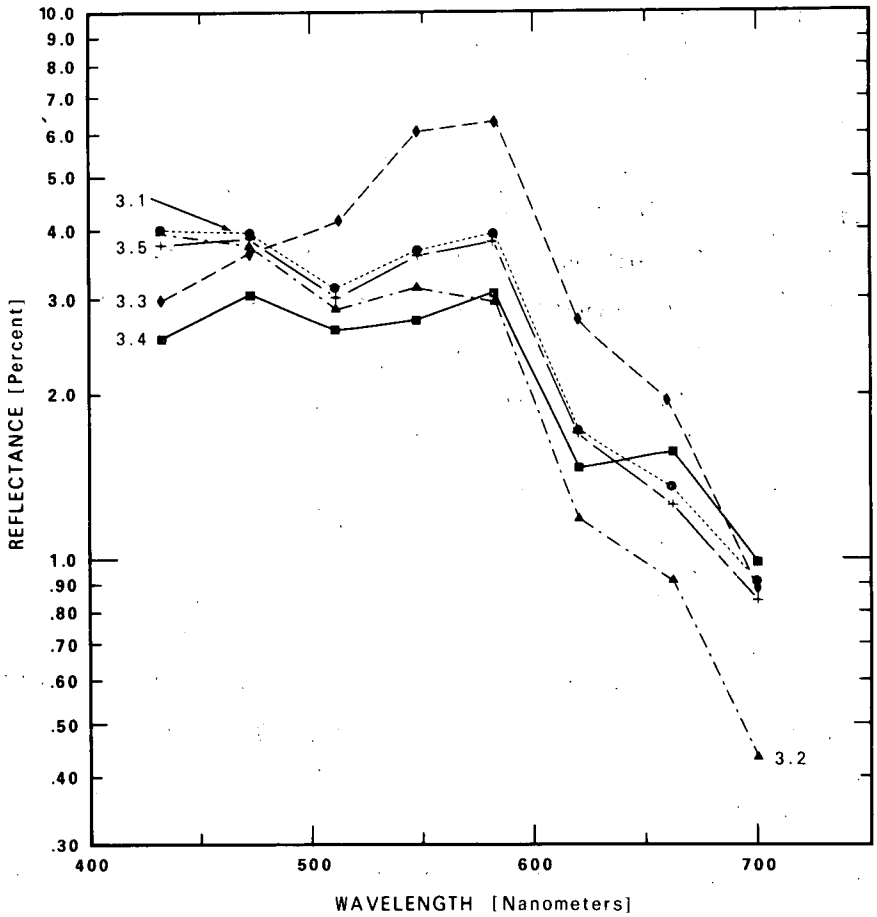


Fig. 13. Computed reflectances for stations 3.1-3.5.

Two final steps of processing are required before considering chlorophyll and sediment algorithms. The location of stations on the OCS imagery requires careful measurement and computation. A program was written to indicate which pixel was located at a particular longitude and latitude. It was during these computations that the best estimate of scan line spacing of 79 meters was obtained. A major point of interest (the acid dump) lies a considerable distance from the only reference location at the north end of the track line. The known fact that the KELEZ was in or near the acid dump for station 3.3 set the scan line spacing given the location of Sandy Hook in the imagery. Figure 14 shows the location of the ship KELEZ and the helicopter stations superimposed on the imagery for channel 4.

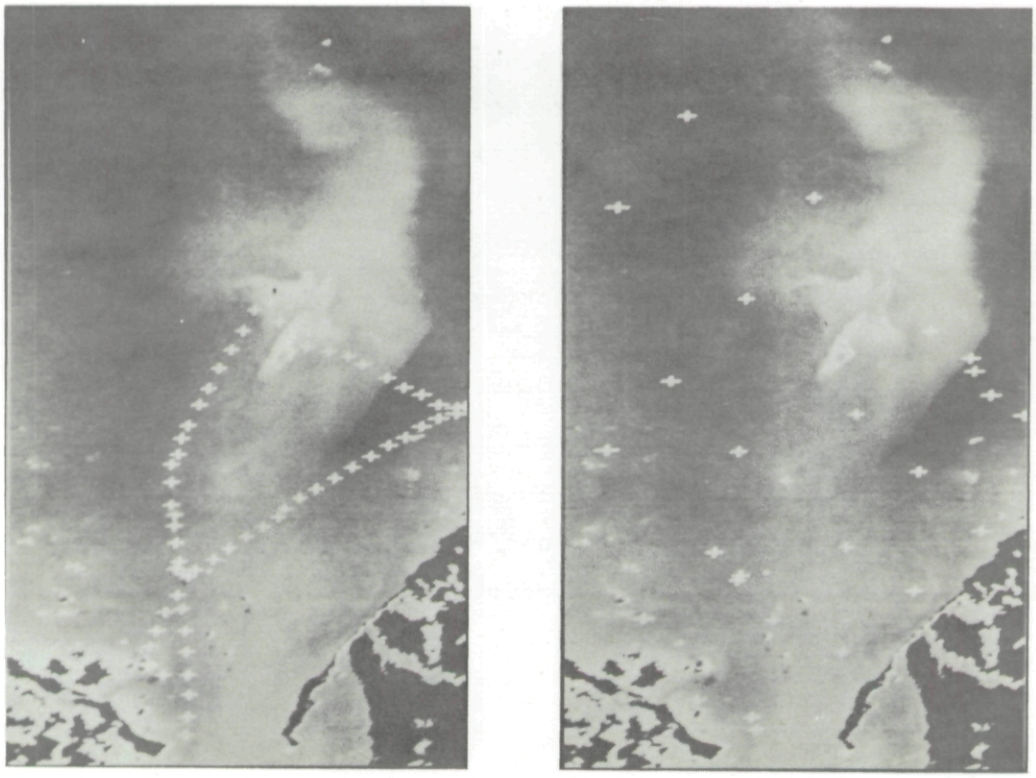

Fig. 14. Image of channel 4 with position of helicopter stations (right image) and KELEZ ship track (left image).

Because of the noisy nature of the data and possible position error, a low pass spatial filter was used on the imagery when values were taken from them. This filter was gaussian shaped with standard deviation of 4 pixels. This filtering essentially performs a local averaging around each pixel. For large arrays and circular spatial averaging this method is faster and more accurate than normal box-car averaging procedures. The actual computation required the Fourier transform of the imagery, multiplication by the gaussian filter function and then the inverse Fourier transform.

## CHLOROPHYLL AND SEDIMENT ALGORITHM

Most previous attempts at deriving algorithms for the chlorophyll-a and sediment concentrations have made direct use of the apparent radiances from the OCS imagery without atmospheric correction. The methods have

basically used an iterative procedure to choose those apparent radiances or ratios of the apparent radiances which best fit the observed chlorophyll-a or sediment concentrations. The problem involved with these heuristic approaches has been the difficulty of transferring these algorithms to other times and/or places. This problem arises because the algorithm so devised need have little or no relationship to the actual physical or biological processes acting in the water column and/or atmosphere.

It was with these thoughts in mind that the procedure partially outlined above was employed. The imagery from the OCS (i.e., apparent radiances) was reduced to a hydro-optical quantity - the subsurface irradiance reflectance R. This quantity was then further reduced to components describing the optical characteristics of the water column.

The basis for the reduction of R was from previous work by Duntley et al. (1974), Morel (1977), Smith & Baker (1977, 1978a,b), and Kiefer & Wilson (1978). In these works and especially the ones by Smith and Baker, it has been shown that the absorption and backscattering properties of chlorophyll-a for a variety of phytoplankton is spectrally conservative. This means that the spectral shape of, say the absorption of chlorophyll-a, is fixed and only its magnitude changes as a function of the concentration. This is not to imply that there are not other components in the water column besides chlorophyll like pigments which may exhibit spectral shape changes.

Kiefer and Wilson observed this relation in studies of laboratory grown phytoplankton cultures. They showed how a simple model of reflectance could be constructed by assuming the absorption and backscattering characteristics of phytoplankton were spectrally conservative and that their magnitude depended only on the concentration of chlorophyll. In general, for this one component model (actually there were two, the phytoplankton and the water itself), the form of the relation for

chlorophyll-a concentration as a function of observed reflectance was

$$\text{Chl conc} = \frac{c_1 + c_2 \frac{R(\lambda_1)}{R(\lambda_2)}}{c_3 + c_4 \frac{R(\lambda_1)}{R(\lambda_2)}} \quad , \tag{1}$$

where the $c_i$ were constants derived from the absorption and backscattering properties of water and phytoplankton, and $R(\lambda_i)$ were reflectances measured at two wavelengths, $\lambda_1$ and $\lambda_2$.

This model was partially successful but assumed that any absorption or backscattering due to particles in the water was from the phytoplankton. Thus in general, it did not allow for absorption and backscattering by substances other than chlorophyll like substances or ones which covaried with the chlorophyll like substances.

Morel (1977) approached the problem by separating the absorption and backscattering characteristics of the reflectance and showing how the reflectance would change as a function of the independent variation of the two components.

Smith and Baker then built upon these concepts by showing how the absorption properties of the water column could be characterized by use of the measured diffuse attenuation coefficients, K. They showed that in addition, K, could be reduced to a summation of components attributed to water, chlorophyll and non chlorophyll like substances. Thus

$$K(\lambda) = K_w(\lambda) + K_x(\lambda) + k_c(\lambda) \cdot C_k \quad . \tag{2}$$

where $C_k$ is the concentration of chlorophyll, $k_c$ is the specific attenuation coefficient for irradiance per unit of chlorophyll like pigments, $K_x$

is a component due to additional substances other than chlorophyll like pigments in the water column and $K_w$ is the water component.

In further work, Smith and Baker (1977) then took this decomposition of K and applied it to Morel's model for reflectance. They then showed a relationship between chlorophyll-a concentration and the measured reflectance at three wavelengths.

Essentially, their derivation starts with the reflectance model proposed and verified by Morel from his experimental observations. He showed that the relation

$$R(\lambda) = 0.33 \frac{b'(\lambda)}{a(\lambda)} \tag{3}$$

yielded a reasonably accurate estimate of reflectance given b', the backscattering, and a, the absorption. Smith and Baker then used a relationship between a and K derived by Preisendorfer (1977) to obtain an equation relating R and K.

Thus given

$$a = \frac{3}{4} \frac{K}{1+2R} , \tag{4}$$

one obtains

$$\frac{R(\lambda)}{1+2R(\lambda)} = \frac{4}{9} \frac{b'(\lambda)}{K(\lambda)} \tag{5}$$

The assumption is then made that b', the backscattering can be broken into a component due to scattering by water, $b'_w$, and one due to particulate scattering, $b'_p$. Therefore equations (2) and (5) yield the relationship

$$\frac{R(\lambda)}{1+2R(\lambda)} = \frac{4}{9} \frac{b'_w(\lambda) + b'_p(\lambda)}{K_w(\lambda)+K_x(\lambda)+k_c(\lambda)\cdot C_K} . \tag{6}$$

Given equation (6) Smith and Baker showed that a relation for the chlorophyll concentration as a function of $R(\lambda)$ could be obtained if measurements of $R(\lambda)$ at three wavelengths were available. It was assumed that the quantities $b'_w$, $K_w$ and $k_c$ were known and that the particulate backscattering was of the form,

$$b'_p(\lambda) = \frac{{}_o b'_p}{\lambda^q}$$

where ${}_o b'_p$ is a normalizing constant and q gives the wavelength dependence of the scattering.

The relationship obtained by Smith and Baker was of the form

$$C_K = \frac{K'(\lambda_2)\ F_1(\lambda_1,\lambda_2,\lambda_3) + K'(\lambda_3)\ F_2(\lambda_1,\lambda_2,\lambda_3)\ \rho_3 + K'(\lambda_1)\rho_1}{k_c(\lambda_2)\ F_1(\lambda_1,\lambda_2,\lambda_3) + k_c(\lambda_3)\ F_2(\lambda_1,\lambda_2,\lambda_3)\ \rho_3 + k_c(\lambda_1)\rho_1}\ , \quad (7)$$

where

$$\rho_i = \frac{R(\lambda_i)}{R(\lambda_2)}\ \frac{(1+2\ R(\lambda_2))}{(1+2\ R(\lambda_i))}\ , \quad (8)$$

$$K'(\lambda) = K_W(\lambda) + K_x(\lambda)\ , \quad (9)$$

and $k_c(\lambda)$ is as previously defined in equation (2). The functions $F_1$ and $F_2$ are functions only of wavelength and essentially describe the spectral scattering properties of water (i.e., $\lambda^{-4.3}$) and of particle backscattering ($\lambda^{-q}$). Neglecting second order reflectance, equation (7) could be reduced to the simpler form

$$C_K = \frac{c_1 + c_2 \frac{R(\lambda_3)}{R(\lambda_2)} + c_3 \frac{R(\lambda_1)}{R(\lambda_2)}}{c_4 + c_5 \frac{R(\lambda_3)}{R(\lambda_2)} + c_6 \frac{R(\lambda_1)}{R(\lambda_2)}} \quad (10)$$

This equation was applied to the reflectances derived from the OCS images.

The actual data used in fitting equation (10) were the reflectances from the pixels at the locations of the helicopter stations and stations 3.1 through 3.5. In determining the best fit to the data from the stations it became apparent that there were three stations which were consistently anomalous with respect to the others. Two of these, stations 3.3 and helicopter station 23, were located in or very close to the acid dump. It is apparent, in light of the physical meaning of the coefficients $K'(\lambda)$ and $k_c(\lambda)$ in equation (7), that the water mass in and near the acid dump was different from the rest of the Bight in terms of the spectral relationships of $K_x(\lambda)$ and $k_c(\lambda)$. There were too few stations directly in the dump to solve equation (7) or (10) for the characteristic components $K_x(\lambda)$ and $k_c(\lambda)$ or $c_1$ through $c_6$. However future research in the Bight area with more extensive sampling in the dump area should lead to a determination of the characteristic components for this area.

The third station which was anomalous with respect to the other stations was helicopter station 1. This station was located directly in the mouth of the river and was probably subject to more change during the period of the experiment than any other one due to tidal action and river outflow. The derived chlorophyll algorithm consistently led to under estimation of the chlorophyll-a concentration by factors of 2 to 3 for this station. It was subsequently ignored in any of the algorithm development.

In Figure 15 the measured chlorophyll-a concentration is plotted versus the computed chlorophyll-a concentration derived from a least squares fit of equation (10) to the available data. The fit was reasonable but there was a large deviation, the correlation $r^2$ being .77.

Investigation, however, led to the conclusion that the stations could be divided into two distinct sets. The first set considered of the stations nearest the New Jersey coast. These were helicopter stations 6,

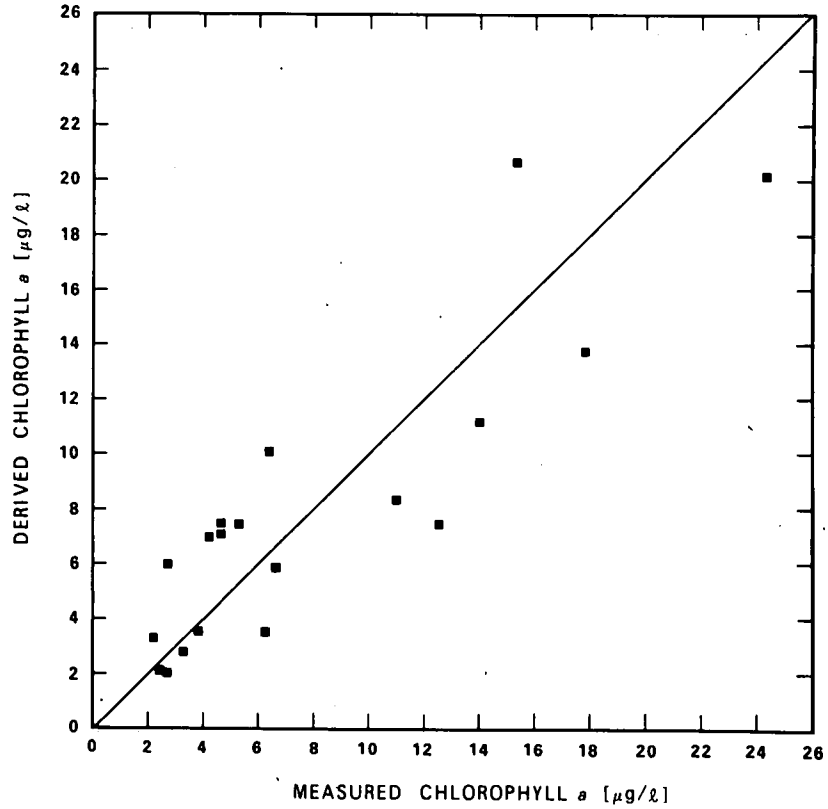


Fig. 15. Measured chlorophyll-a versus derived chlorophyll-a. Derived chlorophyll-a was obtained by a non-linear squares fit of Equation (10) to the available data.

7, 11, 16, 17, and station 3.4. These will be referred to as type one. The rest of the stations (again excluding station 23 and 3.3 in the acid dump) were contained in the other set referred to as type two. If equation (10) was then fitted to these two sets the results in Figures 16 and 17 were obtained. In both of these fits the sum of squares was approximately 5, and the correlation $r^2$ was .99 for the first type (Figure 16) and .97 for type two (Figure 17).

A note should be made with respect to station 3.5. As was observed above, 3.1 and 3.5 were taken at approximately the same location but about 5.5 hours apart in time. The difference in surface chlorophyll-a concentration was on the order of 20%. It was determined in fitting equation (10) to the data that the chlorophyll-a measured at 3.5 was consistently higher than the derived chlorophyll would suggest. In light of the known

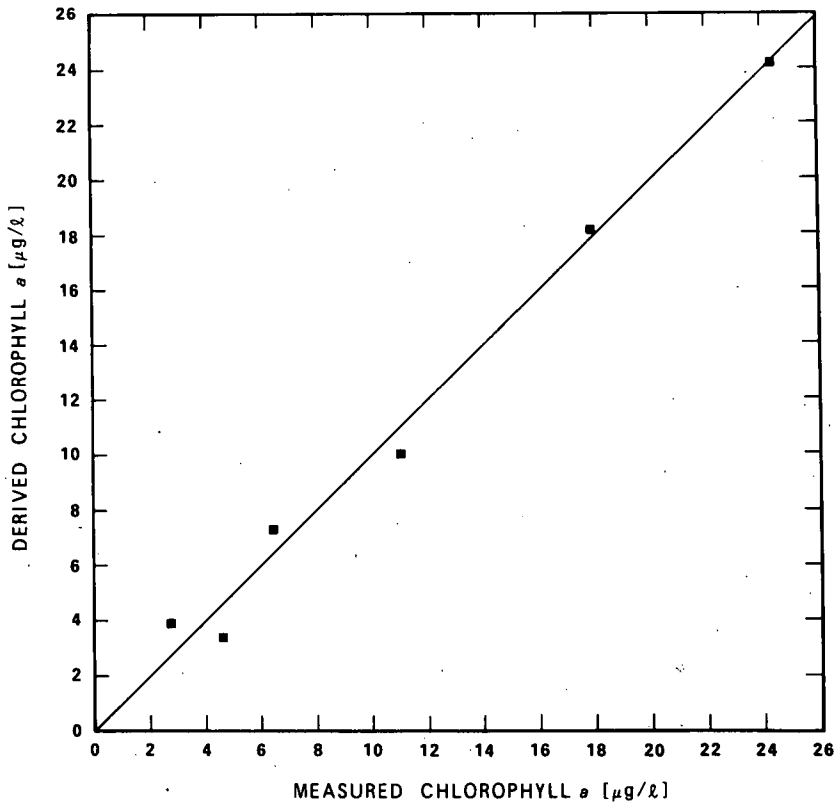


Fig. 16. Measured chlorophyll-a versus derived chlorophyll-a for type one stations. (i.e., those nearest New Jersey coast.)

changes occurring in the chlorophyll-a profile in the region of 3.1 and 3.5, it would seem appropriate to observe that the largest change occurred between the over-flight at 1100 EDT and the measurements taken at station 3.5 at 1419 EDT. Station 3.5 was not used in the least squares fitting in Figure 17. The helicopter stations were made at approximately the time of the overflight.

The equations that gave the best fit to the chlorophyll-a data for the two sets of data are given below.

For the type one stations,

$$C_K = \frac{-1.829 + 2.04\ \rho_3 + 1.226\ \rho_1}{-0.238 + .0057\ \rho_3 + 0.279\ \rho_1}\ , \qquad (11)$$

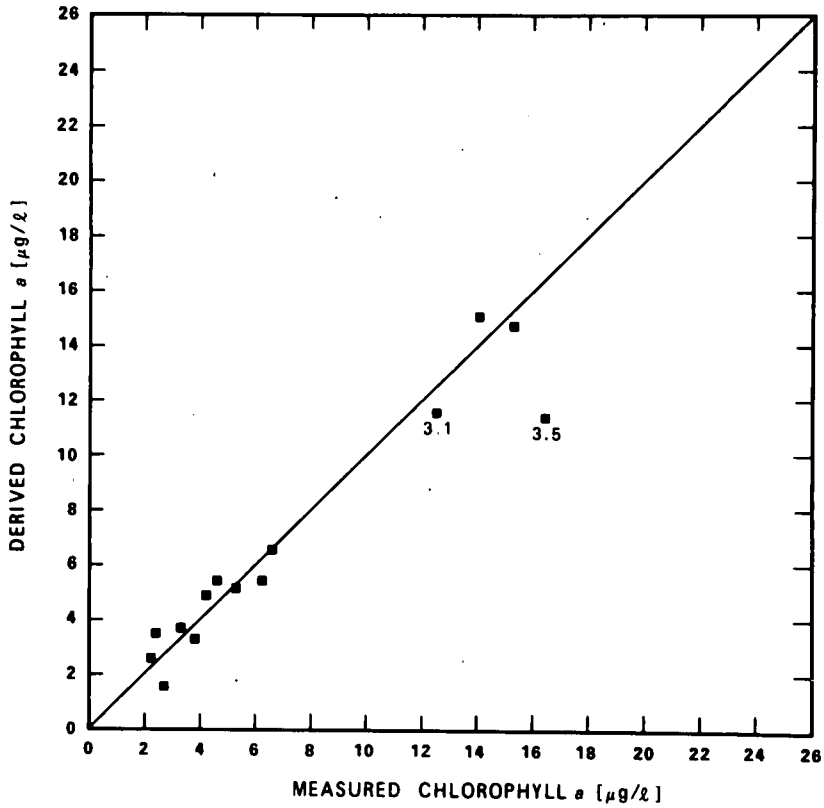


Fig. 17. Measured chlorophyll-a versus derived chlorophyll-a for type two stations. KELEZ stations 3.1 and 3.5 are labeled.

and for the type two stations

$$C_K = \frac{-.465 + 3.46\ \rho_3 + .147\ \rho_1}{-1.08 + .716\ \rho_3 + .848\ \rho_1}\ , \qquad (12)$$

where

$$\rho_1 = \frac{R(471\ nm)}{R(547\ nm)}$$

$$\rho_3 = \frac{R(662\ nm)}{R(547\ nm)}\ .$$

A note of caution should be made with respect to the constants in equations (11) and (12) derived from the least squares fitting. Because

of the small number of samples for each type of water, the degrees of freedom is small. The possible variation of the constants is thus large and the significance of the correlation possibly suspect.

The significance at this stage of research in the development of the algorithm is not so much obtaining the absolute values for the chlorophyll algorithm, but in determining the functional form of the algorithm. If the relationships of the constants in equation (11) and (12) to each other can be traced to similar relationships obtained in other types of water with more samples, then more confidence may be placed on the functional form of the algorithm.

Without independent knowledge of $F_1$ and $F_2$ the fitting of equation (7) to the data, will thus only yield the values of $K'F_1$, $K'F_2$, $k_cF_1$, and $k_cF_2$. This analysis did not allow the estimation of $F_1$ and $F_2$. However, the ratio of $K'/k_c$ may be computed and compared with the results of Smith and Baker.

The values of $K'(=K_w + K_x)$ divided by $k_c$ from Smith and Baker (1978b) for the three wavelengths $\lambda$=461, 547 and 662 nm are plotted in Figure 18 for the two regimes in which Smith and Baker have divided phytoplankton bearing waters. The first regime is where the detrital material in the water column is not correlated with the chlorophyll-a concentration. This type of water in which the chlorophyll-a tends to be higher than in the second group has lower values of $k_c$ and higher values of the $K_x$ component. The second grouping is one in which any detrital material present in the water column has a high correlation with the chlorophyll-a concentration. The diffuse attenuation coefficient $k_c$ for chlorophyll like pigments is thus relatively high and includes a large component due to the detrital material.

The values for $K'/k_c$ for the two sets of stations are also plotted in Figure 18. Smith and Baker note in their work that the values for $K'/k_c$ in the red region of the spectrum may have substantial error due to the limited amount of data available in this region. This comparison of the values of $K'/k_c$ verifies that the division of the stations into two

groups was probably valid and that two distinct types of waters similar to those proposed by Smith and Baker were present in the Bight on April 13. It also indicates, as expressed above, that the functional form of equation (7) may be used in this study with some confidence. The establishment of higher significance on the correlation of derived to measured chlorophyll-a and reduction of the deviation of the constants in equation (11) and (12) requires further study.

Figure 18 indicates that the stations near the New Jersey Coast had relatively high concentrations of chlorophyll-a pigments and a high detrital material content which did not co-vary with the chlorophyll content. Conversely the stations in the rest of the Bight had waters where the detrital material had an appreciable effect on the $k_c$ term and thus co-varied strongly with the chlorophyll content.

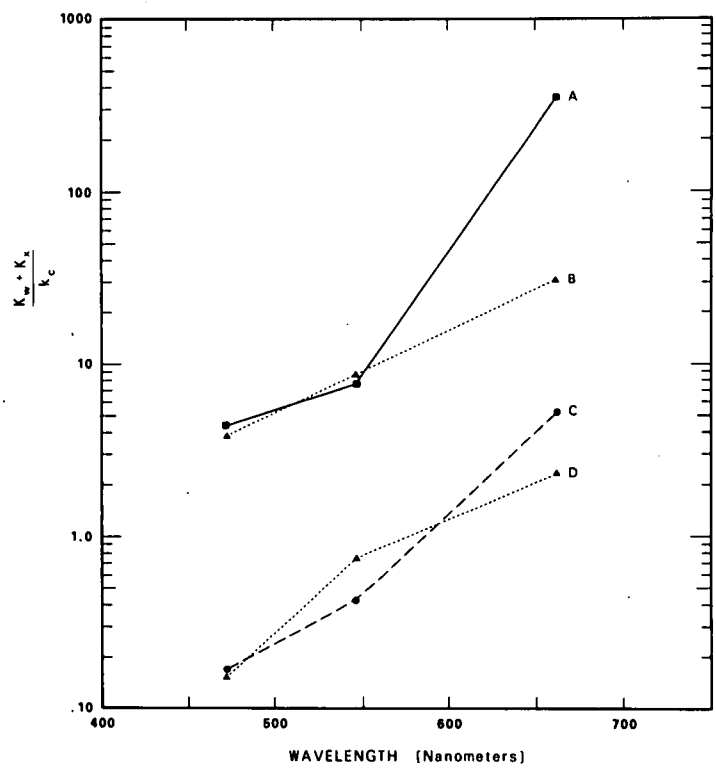


Fig. 18. Plot of the ratio $K_w + K_x$ to $k_c$ versus wavelength. Curve B is data from Smith and Baker for type one water. (i.e., detrital material is not correlated with chlorophyll-a concentration.) Curve A is data from New York Bight, type one stations (Equation 11). Curve D is data from Smith and Baker for type two waters. (i.e., detrital material is correlated with chlorophyll-a concentration.) Curve C is data from New York Bight, type two stations (Equation 12).

Thus from this analysis, it is apparent that the waters in the New York Bight region on 13 April 1975 fell into three distinct water types. First the type that existed near shore on the New Jersey coast. It typically had a high chlorophyll-a concentration but also a high concentration of suspended particular material varying independent of the chlorophyll concentration. This material could be detrital from biological processes but because of the proximity of the shore and the Hudson River it is more likely suspended pollutants and/or river discharge.

The second water type comprised most of the rest of the Bight. This type typically had lower chlorophyll levels than the coastal region and also a detrital material content which was a function of the chlorophyll content. The material was probably connected with the phytoplankton growth cycle either as nutrients and/or direct waste products.

The third water type was found in the acid dump area. Though no estimates could be made of the $K'/k_c$ ratios, this water type should be recognized and not combined with the other two types.

Returning to Figure 13 which is a plot of the reflectance values for stations 3.1-3.5, the typical reflectance curves for the three water types may be observed. Stations 3.1, 3.2, and 3.5 are typical of the type two water. Characteristically they have high blue reflectances and low red ones. Station 3.3 in the middle of the acid dump has a low blue reflectance, very high green-yellow reflectance and an intermediate red value. The number one type of water found off the New Jersey coast is typified by station 3.4. Here the blue reflectance is low while the red is higher than type two.

It is fairly difficult to make a contour map of chlorophyll concentration when the region contains two or more water types. Figure 19 was made by choosing one of the two water types dependent on the relative ratio of the red reflectance to the blue reflectance. From analysis of the data in Figure 13 and similar plots from some of the other stations, a

value of .5 and higher for R(662 nm)/R(471 nm) ratio seemed to indicate type one waters. This criterion was used in generating Figure 19. It was necessary to perform local averaging in Figure 19 to filter out considerable noise in the original map. This local averaging used regions of 7x7 pixels surrounding each pixel for this smoothing.

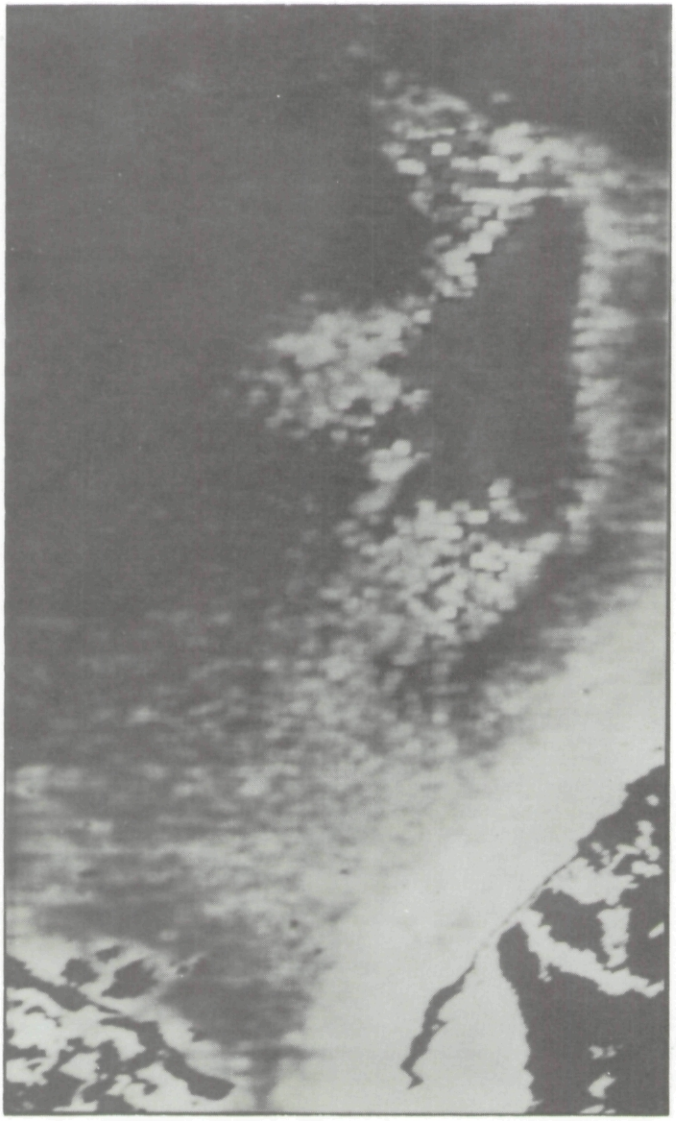

Fig. 19. Map of the derived surface chlorophyll-a concentration in the New York Bight on April 13, 1975. The brightness of the image is linearly proportional to the chlorophyll-a concentration. The brightest value in the map (located inside the river entrance) corresponds to a chlorophyll-a level of 40 $\mu g/\ell$. The region around the acid dump has been set to a nominal low value. The bright ring around this area is due to the failure of the algorithm to take into account the acid dump type water. The application of the algorithm to the acid dump regions yields values of chlorophyll-a from negative to very large (i.e., hundreds) while surface truth data indicates fairly low values.

The area around the acid dump has been set to a nominal value. The algorithms developed above do not give realistic values in this regions (i.e. negative chlorophyll-a concentrations). The development of an algorithm for this type of water must wait on further measurement in this region.

In Figure 20 a histogram of the chlorophyll-a concentration for the region of the Bight in the imagery of Figure 6 is shown. The area around the acid dump has been excluded from the computation. The area under this graph times the total surface area in the imagery of the Bight ($2.4 \times 10^9 m^2$) gives a value for the chlorophyll-a per meter of $14.1 \times 10^6$ gm/m. Assuming an average attenuation depth of 2 meters from which the remote signal is being generated this yields an estimate of total chlorophyll-a in the surface layers of the Bight of $28 \times 10^6$ gms. This estimate, but more importantly this method, of determining the total chlorophyll should be useful in monitoring the productivity of the Bight or any other region.

At the present stage of research in remote sensing of oceanic properties by optical methods, it is premature to talk in quantitative terms of a sediment algorithm. The problem is complicated by the ambiguity of the definition of sediment. It is probably more accurate to talk about the total suspended material in the water column.

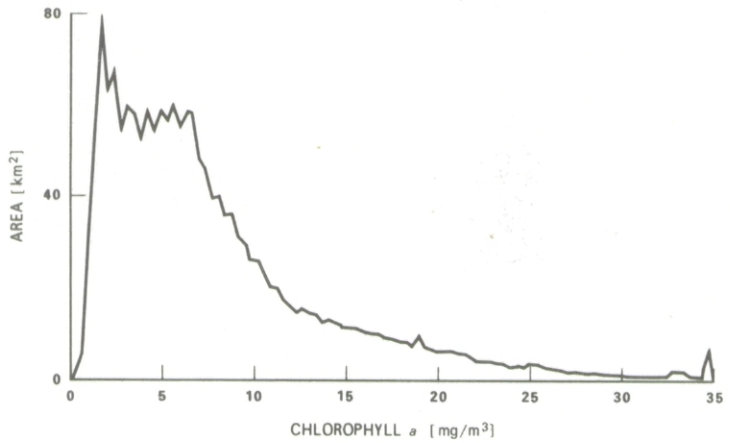


Fig. 20. Area histogram of surface chlorophyll in New York Bight area. A $K^{-1}$ optical depth of 2 meters was chosen as the depth at which the remote signal was being generated.

In biologically dominated waters away from coastal regions, the suspended material in the water may be thought of in terms of the detrital products of the food chain. In these regions the total suspended material will probably co-vary in some manner with the total chlorophyll in the water column.

On the other hand, in coastal waters and especially near the entrance to rivers or harbors, there may be considerable amounts of suspended materials due to river run-off and/or shore wave action. This material may have little or no correlation with the chlorophyll content of the water column. In these regions the diversity of the suspended material content due to the variety of possible sources will probably preclude the development of a single suspended material algorithm for general remote sensing.

However, in any given region it should be possible to characterize the total suspended material in terms of its absorbing and scattering properties. This description could then be used in that region for future monitoring.

Because in most waters, the total suspended material is mainly wavelength neutral (i.e., it scatters light but has little wavelength dependent absorption), the remote optical measurement of the material in the water column will rely chiefly on the monitoring of its backscattering characteristics.

In the development of the chlorophyll algorithm above, it was assumed that the backscattering in the water was composed of two parts. The first part was that due to the water itself and was characterized by a wavelength dependency of $\lambda^{-4.3}$ (Morel). The second part was attributed to particle scattering and had a dependency of $\lambda^{-q}$ where q is of the order 0 to 1 (Morel).

Taking equation (6) and rearranging, the equation below is obtained.

$$b_p' = \left( \frac{9}{4} + \frac{R}{1+2R} \right) \cdot \left( K_w + K_x \right) - b_w' + \left( \frac{9}{4} \frac{R}{1+2R} \right) k_c C_k \, . \qquad (13)$$

This may be rewritten as

$$b_p' = S_0 + S_1 C_k \tag{14}$$

where

$$S_0 = \left( \frac{9}{4} \cdot \frac{R}{1+2R} \right) \cdot \left( K_w + K_x \right) - b_w' \tag{15}$$

$$S_1 = \left( \frac{9}{4} \frac{R}{1+2R} \right) \cdot k_c \tag{16}$$

Thus in the analysis of the chlorophyll algorithm, the assumption that the particulate backscattering is a linear function of the chlorophyll concentration was made.

This assumption is probably not valid in general, especially in waters which may have a substantial terrigeneous based suspended material land. In biologically dominated waters, however, the assumption is reasonable.

If further, the first order assumption that the particle backscattering is proportional to the total suspended material is made, then an equation of the form of equation (14) is obtained.

Therefore,

$$S = S_0' + S_1' C_k \tag{17}$$

where S is the total suspended material.

Again this proportionality will be highly dependent on the size distribution and scattering efficiency of the suspended particles. The main justification at this stage for the assumption is to illustrate the possible relationship between the chlorophyll concentration and the total suspended material.

If a plot of total suspended material versus surface chlorophyll for the whole New York Bight is made and equation (19) fitted to the data,

values for $S_0'$ and $S_1'$ of 0.0741 and 0.3146 are obtained. The correlation $r^2$ is 0.81.

Though the correlation is fairly low, the result does indicate the trend of the relationship. The largest scatter occurs at the higher chlorophyll values and for those points in the type one water (i.e., those close to the New Jersey coast). As observed above, this water type probably contained a large quantity of suspended material non-biological in character.

In this analysis since the total suspended material concentration is linear with respect to the chlorophyll concentration, the chlorophyll map of Figure 19 will also give the approximate distribution of total suspended material.

Much further work needs to be done in the Bight area with respect to the relationship of the suspended material to the optical signal generated by it. Because of the variability of the content of the suspended material in the Bight due to the proximity to the Hudson River and near by heavily populated coastal areas, it may not be possible to obtain a general suspended material algorithm along the lines of the chlorophyll one.

Further, in-situ measurements of the reflectance of the waters in the Bight along with suspended material measurements over several seasons and under varying oceanic conditions need to be made in order to establish a data base from which any general conclusions may be made.

## SUMMARY

The effectiveness of remote sensing by use of the OCS has been demonstrated above. The high correlations between the computed chlorophyll-a concentration and the actual measured ones show the necessity of removing the effects of the atmosphere from the OCS imagery. The correlations obtained are higher than those obtained using other methods not employing atmospheric corrections.

The form of the chlorophyll algorithm used also has significance in the sense that the coefficients may be reduced to parameters directly related to the absorbing-scattering properties of the water, particles, and chlorophyll like pigments. Parameters with physical meaning are vital in using the algorithm at other times and locations. Knowledge of the optical properties of natural waters along the lines demonstrated by Smith and Baker should give the coefficients necessary for use of the algorithm for other places.

Another significant aspect of the analysis is the illustration of the variability encountered in relating surface measurements made over a period of time to a synoptic measurement from a platform such as the U-2. The variations seen at stations 3.1 and 3.5 show that simultaneous measurements need to be made in order to reduce the scatter of data. It should be recognized that the variation observed between the OCS imagery and surface measurements in past work may be due to this lack of similarity.

One of the most significant aspects of the analysis is that different water types do exist in a relatively small area such as the New York Bight. The grouping of the whole area under one type is a simplistic view and one which will probably cause failure of algorithms to work over extended areas and/or times.

Though the overall result of the analysis has been satisfactory, further research is needed in several areas. Basically, the chlorophyll analysis was done at three wavelengths. The form of the analysis was such that more detailed information about the values of coefficients $k_c$ and $K_x$ was lacking. Further research and work utilizing the three wavelengths and possibly one other should yield more knowledge of these values.

In order to type the water found in the acid dump, further measurements need to be made in this area. These would be sub-surface reflectance and attenuation measurements similar to ones Smith and Baker used. For that matter these types of underwater optical measurements throughout the Bight area would yield significant insight into the form

and substance of equation (7) for use not only in the area but extrapolation to other regions as well.

## ACKNOWLEDGEMENTS

This work has been supported by funding from the U.S. Department of Commerce, National Oceanic and Atmospheric Administration, National Environmental Satellite Service under Grant 04-6-158-44033.

The author wishes to thank Jack Sherman and Dennis Clark of NOAA-NESS for their assistance. Also discussions with Dr. Raymond Smith, Dr. Dale Kiefer, Roswell Austin and Karen Baker were most beneficial.

## REFERENCES

Duntley, S. Q., R. W. Austin, W. H. Wilson, C. F. Edgerton, and S. E. Moran, "Ocean Color Analysis", SIO Ref. 74-10 (1974).

Gordon, H. R. and W. R. McCluney, "Estimation of the Depth of Sunlight Penetration in the Sea for Remote Sensors", Applied Optics 14, 413-416 (1975).

Gordon, J. L., "Model for a Clear Atmosphere", J. Opt. Soc. Amer. 59, 14-18 (1969).

Gordon, J. L., "Directional Radiance (Luminance) of the Sea Surface", SIO Ref. 69-20 (1969).

Hovis, W. A. and K. C. Leung, "Remote Sensing of Ocean Color". Optical Engineering 16, 158-166 (1977).

Kiefer, D. A., "Fluorescence Properties of Natural Phytoplankton Populations", Marine Biology 22, 263-269 (1973).

Kiefer, D. A. and W. H. Wilson, "Reflectance Spectroscopy of Marine Phytoplankton", SIO Ref. 78-6 (1978).

Morel, A. and L. Prieur, "Analysis of Variations in Ocean Color", Limnology and Oceanography 22, 709-722 (1977).

Preisendorfer, R. W., Hydrologic Optics, NOAA-ERT (1977).

Selby, J. E. A. and R. A. McClatchey, "Atmospheric Transmittance from 0.25 to 28.5 μm: Computer Code LOWTRAN 3", Air Force Cambridge Research Laboratories, AFCRL-TR-75-0255 (1975).

Smith, R. C. and K. S. Baker, "Remote Sensing of Chlorophyll", Proceedings of XXth Meeting COSPAR "Symposium on the Contribution of Space Observations to Global Food Information Systems" (1977).

Smith, R. C. and K. S. Baker, "The Bio-Optical State of Ocean Waters and Remote Sensing", Limnology and Oceanography 23, 247-259 (1978a).

Smith, R. C. and K. S. Baker, "Optical Classification of Natural Waters", Limnology and Oceanography 23, 260-267 (1978b).

Thekaekara, M. P., "Extraterrestrial Solar Spectrum, 3000-6100 Å at 1° Intervals", Applied Optics 13, 518-522 (1974).

Wilson, W. H., "Radiative Transfer Modeling in an Oceanic-Atmospheric System - RADSEA", in preparation (1979).